Modeling of Monolithic RF Spiral Transmission-Line Balun

Yeong J. Yoon, Yicheng Lu, Robert C. Frye, and Peter R. Smith

***Abstract*—This paper presents models for monolithic RF spiral transmission-line baluns. The balun consists of a pair of spiral transformers fabricated on high-resistivity silicon. The lumped-element equivalent models are developed. The second–order or higher order models are synthesized from the first-order lumped model. All lumped parameters for the models are extracted from the real physical structures. Simulated behaviors from the second-order models are in good agreement with the measured results within 10% difference.**

***Index Terms*—Balun, lumped model, spiral transformer, transmission line.**

I. Introduction

Baluns are devices that provide balanced outputs from an unbalanced input. There are 180° out of phase and half the input signal amplitude at the two output terminals. RF baluns find important applications in double-balanced mixer circuits and matching networks between antennas and low-noise amplifiers (LNAs). Compensated Marchand baluns [1], which are made of two transmission lines, furnish excellent balanced outputs over a wide frequency range. Marchand-type baluns in simple transmission-line forms have been successfully adapted in double balanced mixer designs [2]. Chen *et al.* [3] reported a balun lumped model by using a curve-fitting technique on measurements. However, such an empirical model is difficult to correlate with new or modified designs since it does not directly link to the physical parameters of the baluns. Complicated analytic formulas for Marchand-type baluns have been reported [4], but the extension to lumped model is not obvious. In this paper, we describe first- and second-order equivalent lumped models for spiral baluns based on physical design parameters, instead of on empirical extraction from measurements. The model can be easily extended to the higher orders. The simulation results are compared with measurements for spiral transmission-line baluns.

II. Balun Structure

The detailed operating principle of the general transmission-line balun, as shown in Fig. 1(a), can be found elsewhere [1], [5]. Shown in Fig. 1(b) is the spiral balun composed with two nested spiral pairs or spiral transformers. The electrical lengths of all conductors are approximately equal to $\lambda/4$ at the center of the frequency band. The layout is basically a spiral version of the coupled transmission-line balun. The two inner end points of the coils are tied together to a common ground point. By using this arrangement, the spiral coils are symmetric with respect to the ground connection. The potentials at short-circuit connections in Fig. 1(a) are the same due to the symmetrical design, which minimizes the output imbalance [6], even though the return current path through the ground frame has certain inductance. Thus, the lumped-element model can be developed with respect to the common ground point.

Manuscript received August 26, 1999.

Y. J. Yoon is with SyChip Inc., Lucent Technologies Venture, Murray Hill, NJ 07974-0636 USA.

Y. Lu is with the Department of Electrical and Computer Engineering, Rutgers University, Piscataway, NJ 08854-8058 USA (e-mail: ylu@ece.rutgers.edu).

R. C. Frye and P. R. Smith are with Lucent Technologies, Murray Hill, NJ 07974-0636 USA.

Publisher Item Identifier S 0018-9480(01)01085-7.

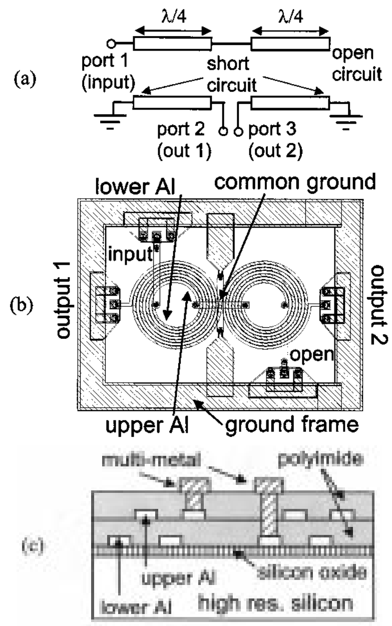

Fig. 1. (a) Schematic representation of a transmission-line balun. (b) Layout of a spiral transmission-line balun consisting of two spiral transformers. The coplanar ground frame provides the return path for current. (c) Cross-sectional view of the spiral transformer.

The substrates are high resistivity (>4000 $\Omega \cdot$cm) silicon with a 1-μm thickness of thermally grown silicon dioxide for added electrical isolation. A polyimide layer with the thickness of approximately 3.5 μm serves as an insulator between two 3-μm-thick Al metal layers. The two Al coils are offset vertically, as shown in Fig. 1(c). The third metal layer, on the top of the second polyimide, is a 1-μm-thick multilayer of Cr–CrCu–Cu–Au, which is used to form the bridges between the inner and outer parts of the spirals.

III. Results and Discussion

A. Lumped-Element Models

Practical spiral inductors can be approximated by a lumped equivalent model including resistance R, inductance L, capacitance to ground C_g, and capacitance across the spiral inductors C_I, which consists of self-wound capacitance and capacitance by the crossover between inside and outside of the coils. Conductance through the substrate is neglected due to its high resistivity. The lumped model for the spiral transformer must include the mutual inductance L_m and mutual capacitance C_m. The first-order model [7] excludes C_g for simplicity and C_m is divided equally between the two ends of the spirals. L_m is represented by dependent voltage sources.

The computation methods of the inductance and resistance for a spiral structure have been described in many references, e.g., in [7] and [8]. Due to the difficulties arising from the vertically skewed Al coils, as depicted in Fig. 1(c), we used a two-dimensional field solver [9] for the cross section of the balun to find the mutual capacitance per unit length between adjacent lines of the upper and lower coils. The self-wound capacitance is often negligibly small, and the parallel-plate capacitor method is employed to estimate the crossover capacitance. The structures of the baluns have coplanar ground frames, as shown in Fig. 1(b). The capacitance per turn to ground becomes smaller due to

TABLE I
DESIGN PARAMETERS, LUMPED VALUES, AND ESTIMATION METHODS

Width	Spacing	Inner Radius	Turns	Length
30 μm	40 μm	200 μm	4.5	1.01cm
Parameters	Values	Method		
L, L_m (nH)	17.7, 13.9	formulae in [7,9]		
C_m (pF)	1.05	2 Dimensional field solver		
C_g (pF)	0.11	CPS formulae [10,11] for 2 outer turns		
C_I (pF)	0.03	used parallel plate capacitor formula		
R(Ω)	3.41	formula in [8]		

the shielding effect as the conductor turns progress inward toward the center of the spiral. We numerically found that reasonable C_g values can be obtained by considering only the two outermost turns. The cross section of the ground frame and the outer turn may be approximated by a coplanar stripline (CPS). Thus, C_g is estimated by using both of the effective dielectric-constant equations for the multilayered system [10] and the asymmetric CPS capacitance formula [11]. The spiral geometry and calculated lumped values including estimation methods are listed in Table I.

The second-order equivalent model of the transformer can be synthesized as depicted in Fig. 2 by two series-connected first-order models, where all lumped values, except the mutual inductive coupling coefficient k are equally distributed. The higher order models can be obtained by further expansion. By considering the schematic representation in Fig. 1(a), the second-order or higher order lumped model for the balun can be completed by appropriate connections between two models of the spiral transformers. Since all lumped values are developed based on the physical design parameters, the models can correspondingly predict the characteristics by using a circuit simulator, e.g., Libra in HP EEsof [12] when the design changes.

B. Simulation and Analysis

The S_{11} curve in Fig. 3(a) from the first-order model has input matches around 1.5 and 3.2 GHz. The predicted bandwidth, determined by the conventional 3-dB method, is approximately from 0.9 to 3.1 GHz. The second-order model gives the bandwidth from 0.9 to 4.1 GHz, as shown in Fig. 3(b). At the frequencies of 1.6 and 3.7 GHz, the input reflection with a 50-Ω source is simulated lower than 25 dB. From the measured S_{11} curve of Fig. 3(c), it can be seen that input matching for the 50-Ω source is lower than 23 dB at the frequencies of 1.6–3.5 GHz. The measured 3-dB bandwidth ranges from 0.83 to 4.17 GHz, which is quite close to the simulation results from the second-order model. Around 5 GHz, the simulation in Fig. 3(b) displays an apparent additional resonance, whereas in the measurement, this is smeared out because of the distributed nature of the balun.

From Fig. 4(a), the simulation from the second-order model accurately predicts the phase behavior up to 1.6 GHz, above which frequency the predicted and measured phase behaviors begin to depart. Up to 3.2 GHz, the difference between simulated and measured phase angle is less than 4°. The center frequency of 3-dB bandwidth and the amplitude imbalance between simulation and measurement from [13] are illustrated in Fig. 4(b). The simulated center frequencies differ from the measurement by less than 7%. The amplitude imbalance from the simulation separates as low as 0.5 dB at maximum with the measurements for 50-μm-metal-width baluns.

A spiral structure is not electrically uniform along its conductor length, and the coupling between the nested spiral lines is complicated, resulting in difficulties in obtaining the exact lumped values. It is found that the second-order lumped model is good enough to describe the spiral transmission-line balun properties as higher order models

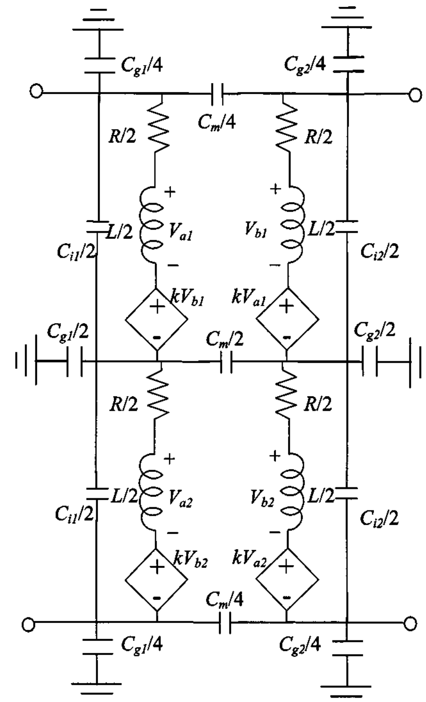

Fig. 2. Second-order equivalent lumped model of the spiral transformer. The model is synthesized by two series-connected first-order models shown in [7] including capacitance to ground. The lumped values are equally distributed over the model.

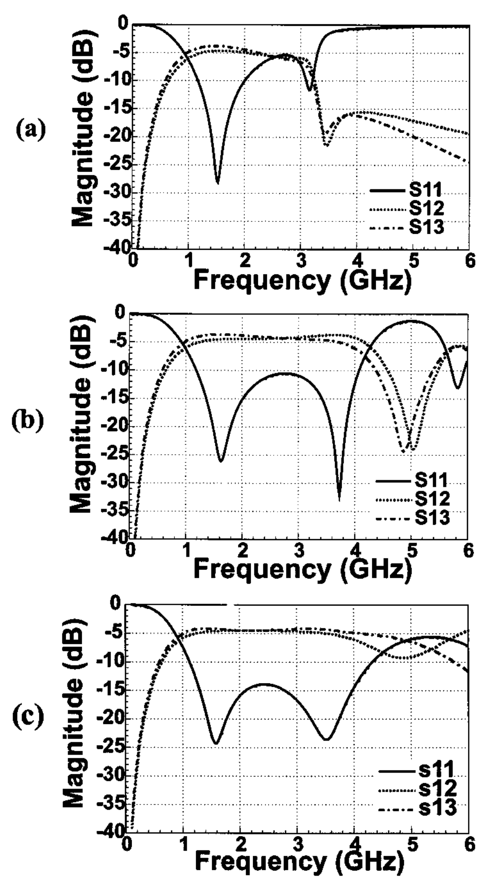

Fig. 3. Magnitude of S-parameter response from: (a) the first-order model, (b) the second-order model, and (c) the measurement.

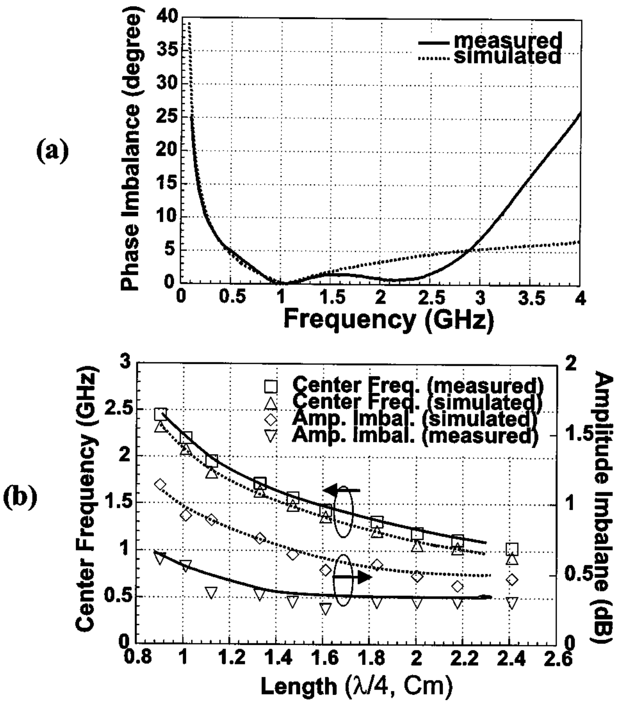

Fig. 4. Comparison of: (a) simulated phase deviation with measurement for the spiral transmission-line balun and (b) simulation with measurement in terms of frequency of bandwidth and amplitude imbalance for 50-μm-conductor-width baluns built on high-resistivity silicon substrates.

beyond the second order slightly improve the accuracy with the price of high model–circuit complexity.

IV. Conclusions

In this paper, we have presented the first- and second-order equivalent lumped-element models for spiral transmission-line baluns. The second-order and higher order models are synthesized from the first-order model. Since the model parameters are based on lumped values extracted from the physical structures of the devices, the models are useful for predicting the major characteristics from the design parameters of baluns. In comparison with the measurement results, the second-order model captures all important features of the behaviors of the spiral couplers and transmission-line baluns within 10% error.

References

[1] N. Marchand, "Transmission line conversion transformers," *Electronics*, vol. 17, pp. 142–145, Dec. 1944.

[2] W. R. Brinlee, A. M. Pavio, and K. R. Varian, "A novel planar double balanced 6–18 GHz MMIC mixer," in *IEEE MTT-S Int. Microwave Symp. Dig.*, 1994, pp. 9–12.

[3] T. Chen, K. W. Chang, S. B. Bui, H. Wang, G. Samuel, L. C. T. Lui, T. S. Lin, and W. S. Titus, "Broad-band monolithic passive baluns and monolithic double-balanced mixer," *IEEE Trans. Microwave Theory Tech.*, vol. 39, pp. 1980–1986, Dec. 1991.

[4] M. Engels and R. H. Jansen, "Design of integrated compensated baluns," *Microwave Opt. Technol. Lett.*, vol. 14, no. 2, pp. 75–81, 1997.

[5] W. K. Roberts, "A new wide-band balun," *Proc. IRE*, vol. 45, pp. 1628–1631, Dec. 1957.

[6] Y. J. Yoon, Y. Lu, R. C. Frye, and P. R. Smith, "A silicon monolithic spiral transmission line balun with symmetrical design," *IEEE Electron. Device Lett.*, vol. 20, pp. 182–184, Apr. 1999.

[7] ——, "Spiral transmission line baluns for RF multi-chip module packages," *IEEE Trans. Comp., Packag., Manufact. Technol.*, vol. 22, pp. 332–336, Aug. 1999.

[8] E. Pettenpaul, H. Kapusta, A. Weisgerber, H. Mampe, J. Lugunsland, and I. Wolff, "CAD models of lumped elements on GaAs up to 18 GHz," *IEEE Trans. Microwave Theory Tech.*, vol. 36, pp. 294–304, Feb. 1988.

[9] *Transmission Line and Crosstalk Products User's Manual, XNS-TLC-XFX*, Mentor Graphics, Wilsonville, OR, 1996.

[10] E. Chen and S. Y. Chou, "Characteristics of coplanar transmission lines on multilayer substrates: Modeling and experiments," *IEEE Trans. Microwave Theory Tech.*, vol. 45, pp. 939–945, June 1997.

[11] K. C. Gupta, R. Grag, I. Bahl, and P. Bhartia, *Microstrip Lines and Slotlines*, 2nd ed. Norwood, MA: Artech House, 1996, ch. 7.

[12] *Libra Reference Manual in HP EEsof Series IV*, Hewlett-Packard, Santa Rosa, CA, 1996.

[13] Y. J. Yoon, Y. Lu, R. C. Frye, M. Lau, P. R. Smith, L. Alquist, and D. Kossives, "Design and characteristics of multilayer spiral transmission line baluns," *IEEE Trans. Microwave Theory Tech.*, vol. 47, pp. 1841–1847, Sept. 1999.

Transmission-Line Stabilized Monolithic Oscillators

Kian Sen Ang, Michael J. Underhill, and Ian D. Robertson

***Abstract*—A novel technique for frequency stabilization and phase-noise reduction of monolithic oscillators is presented in this paper. It employs simple transmission-line resonators, which are many wavelengths long to increase the oscillator quality factor. Monolithic oscillators at 20 and 40 GHz are realized for the application of this technique. Phase noise reduction of more than 20 dB was achieved for both oscillators. The single-sideband phase noise obtained was −100 dBc/Hz at 100-KHz offset for the 20-GHz oscillator and −90 dBc/Hz at 1-MHz offset for the 40-GHz oscillator. The approach is implemented by using readily available transmission lines, which are open- or short-circuited at one end and connected to the monolithic-microwave integrated-circuit (MMIC) oscillator at the other end. Thus, it presents significant potential in the development of low-cost MMIC oscillators with enhanced noise performance.**

***Index Terms*—Frequency stability, MMIC oscillators, phase noise, transmission-line resonators.**

I. Introduction

In recent years, an increasing number of oscillator circuits has been implemented using monolithic technology due to the overwhelming advantages of size, reliability, and cost [1]. These oscillators, however, generally have poor phase-noise performance as the monolithic circuitry has relatively low quality factor (Q). To meet the low noise requirements of practical systems, some form of an oscillation stabilizing scheme has to be employed.

The most common frequency stabilization and phase-noise reduction techniques are the use of dielectric resonator oscillators (DROs) [2], [3] and phase-locked oscillators (PLOs) [4], [5]. Due to the extraordinarily high-Q, DROs offer excellent low noise performance. However, they require accurate dimensions of the dielectric puck and its precise placement on the monolithic or package substrate, as these parameters determine the oscillating frequency and stability. This demands careful

Manuscript received October 4, 1999. This work was supported in part by the Engineering and Physical Sciences Research Council and in part by Prof. K. K. Cheng, Chinese University of Hong Kong. The work of K. S. Ang was supported in part by the Defence Science Organization National Laboratories.

The authors are with the Microwave and Systems Research Group, School of Electronic Engineering, Information Technology and Mathematics, University of Surrey, Guildford, Surrey GU2 7XH, U.K. (e-mail: k.ang@eim.surrey.ac.uk).

Publisher Item Identifier S 0018-9480(01)01086-9.